1 Monoallelic CRMP1 gene variants cause neurodevelopmental disorder

- 2 Ethiraj Ravindran, Nobuto Arashiki, Lena-Luise Becker, Kohtaro Takizawa, Kohtaro Takizawa,
- 3 Jonathan Lévy, 5,6 Thomas Rambaud, Konstantin L. Makridis, 1-3 Yoshio Goshima, Na Li, 8
- 4 Maaike Vreeburg, Bénédicte Demeer, 10, 11 Achim Dickmanns, 12 Alexander P.A Stegmann, 9
- 5 Hao Hu, ^{8*} Fumio Nakamura, ^{4*} Angela M. Kaindl ^{1-3*}

Author affiliations:

- ¹Department of Pediatric Neurology, Charité–Universitätsmedizin Berlin, Berlin, 13353,
- 9 Germany.

6

7

- ²Center for Chronically Sick Children, Charité–Universitätsmedizin Berlin, Berlin, 13353,
- 11 Germany.
- ³Institute for Cell Biology and Neurobiology, Charité–Universitätsmedizin Berlin, Berlin,
- 13 10117, Germany.
- ⁴Department of Biochemistry, Tokyo Women's Medical University, Tokyo, Sinjuku-ku, 162-
- 15 8666, Japan.
- ⁵Department of Genetics, APHP-Robert Debré University Hospital, Paris, 75019, France.
- ⁶Laboratoire de biologie médicale multisites Sequia FMG2025, Paris, 75014, France
- ⁷Department of Molecular Pharmacology and Neurobiology, Graduate School of Medicine,
- 19 Yokohama City University, Yokohama, Kanazawa-ku, 236-0004, Japan.
- ⁸Laboratory of Medical Systems Biology, Guangzhou Women and Children's Medical Center,
- Guangzhou Medical University, 9 Jinsui Road, 510623, Guangzhou, China.
- ⁹Clinical Genetics, Maastricht University Medical Center, Maastricht, 6202, Netherlands.

- 23 ¹⁰ Center for Human Genetics, CLAD Nord de France, CHU Amiens-Picardie, Amiens,
- 24 80054, France

30

41

43

- 25 ¹¹CHIMERE EA 7516, University Picardie Jules Verne, Amiens, France
- 26 ¹²Department of Molecular Structural Biology, Institute for Microbiology and Genetics
- 27 (GZMB), Georg-August-University Göttingen, Göttingen, 37077, Germany
- 29 *, \$, # These authors contributed equally to this work.

31 Corresponding authors:

- 32 Professor Dr. Angela M. Kaindl, Charité Universitätsmedizin Berlin, Campus Virchow-
- 33 Klinikum, Augustenburger Platz 1, 13353 Berlin. Tel / Fax: +49 30 450 566301 /7566301.
- 34 Email: angela.kaindl@charite.de*.
- 35 Professor Fumio Nakamura, Tokyo Women's Medical University, Department of
- 36 Biochemistry, 8-1 Kawada-cho, Sinjuku-ku, Tokyo, Japan. 162-8666 Tel / Fax: +81-3-5269-
- 37 7415. Email: nakamura.fumio@twmu.ac.jp**.
- 38 Dr. Hao Hu, Laboratory of Medical Systems Biology, Guangzhou Women and Children's
- 39 Medical Center, Guangzhou Medical University, 9 Jinsui Road, 510623, Guangzhou, China.
- 40 Tel / Fax: +86 (0)20 38076326/265. Email: huh@cougarlab.org**.
- 42 **Running title:** CRMP1 and neurodevelopmental disorder
- 44 **Keywords:** CRMP1; brain development; intellectual disability; autism spectrum disorder;
- 45 neurodevelopmental disorder.

- **Email addresses:** ethiraj.ravindran@charite.de, arashiki.nobuto@twmu.ac.jp, lena-
- 47 luise.becker@charite.de, takizawa.kohtaro@twmu.ac.jp, jonathan.levy@aphp.fr,
- 48 thomas.rambaud@laboratoire-seqoia.fr, konstantin.makridis@charite.de,
- 49 goshima@yokohama-cu.ac.jp, lina@cougarlab.org, m.vreeburg@mumc.nl,
- 50 demeer.benedicte@chu-amiens.fr, adickma@gwdg.de, sander.stegmann@mumc.nl,
- 51 huh@cougarlab.org, nakamura.fumio@twmu.ac.jp, angela.kaindl@charite.de

Abstract

Collapsing response mediator proteins (CRMPs) are key for brain development and function. Here, we link CRMP1 to a neurodevelopmental disorder. We report heterozygous *de novo* variants in the *CRMP1* gene in three unrelated individuals with muscular hypotonia, intellectual disability and/or autism spectrum disorder. Based on *in silico* analysis these variants are predicted to affect the CRMP1 structure. We further analyzed the effect of the variants on the protein structure/levels and cellular processes. We showed that the human *CRMP1* variants are dominant-negative and impact the oligomerization of CRMP1 proteins. Moreover, overexpression of mutant-*CRMP1* variants affect neurite outgrowth of murine cortical neurons. While altered CRMP1 levels have been reported in psychiatric diseases, genetic mutation in *CRMP1* gene has never been linked to human disease. We report for the first-time mutations in the *CRMP1* gene and emphasize its key role in brain development and function by linking directly to a human neurodevelopmental disease.

Introduction

66

67

68

69

70

71

72

73

74

75

76

77

78

79

80

81

82

83

84

85

86

87

88

89

90

91

Neurodevelopment is a fine-tuned process orchestrated by distinct expression and function of several genes and any disturbances in this timely-controlled process culminate in neurodevelopmental disorder. 1,2 Collapsin response mediator proteins (CRMP) are cytosolic phosphoproteins that are highly and differentially expressed in the nervous system.^{3,4} The five CRMP subtypes (CRMP1-5) form homo- or hetero-tetramers in various combinations and thereby enable distinct functions key for neurodevelopment.⁵ Targeted neurodevelopmental processes include cell migration, axonal outgrowth, dendritic branching, apoptosis mediated through extracellular signaling molecules (Sema3A, reelin, neurotrophins). 6-10 CRMP function is regulated in a spatiotemporal manner through protein phosphorylation mediated by various kinases such as Cdk5, Rho/ROCK, and GSK3. 11,12 Given their key function in developmental processes, disturbances in CRMP function can result in neurodevelopmental diseases (NDD). In this line, monoallelic CRMP5 variants can cause Ritscher-Schinzel syndrome 4 (MIM#619435), a neurodevelopmental disease with craniofacial features, cerebral and cardiovascular malformations, and cognitive dysfunction. 13 CRMP4 variants have been associated with amyotrophic lateral sclerosis in the French population.¹⁴ Here, we link for the first time CRMP1 variants in three unrelated pedigrees to neurodevelopmental disorder in humans with muscular hypotonia, autism spectrum disorder (ASD) and/or intellectual disability. In humans, maternal CRMP1 autoantibodies have been associated with autism in their children, and increased CRMP1 mRNA levels were identified in individuals with schizophrenia, attention deficit hyperactivity disorder and ASD. 15,16 Knockout of Crmp1 in mice results in schizophrenia-associated behavior, impaired learning and memory, and prepulse inhibition.¹⁷ On a cellular level, abnormal neurite outgrowth, dendritic development and orientation, and spine maturation of cortical and/or hippocampal neurons have been shown. 7-9 Loss of Crmp affects long-term potentiation maintenance. 9 In

addition, cerebellar development and its loss leads to reduced granule cell proliferation, apoptosis, and migration in the cerebellum of *Crmp1*^{-/-} mice.¹⁰ Although evidence on altered levels of CRMP1 in neuropsychiatric diseases exists, the mutations in the *CRMP1* gene has

to

a

human

disease.

linked

95

not

been

Subjects and methods

96

97

98

99

100

101

102

103

104

105

106

107

108

109

110

111

112

113

114

115

116

117

118

119

120

Written informed consent was obtained from all parents of the patients to participate in this study and publish the data of this research work. The human study adhered to the World Health Association Declaration of Helsinki (2013) and was approved by the local ethics committees of the Charité (approval no. EA1/212/08). All animal experimental protocols were checked and approved by the Institutional Animal Care and Use Committee of the Tokyo Women's medical University with protocol No. 'AE21-086'. All animal experiments were performed at daytime. The study was not pre-registered. Genetic analyses. In family 1, DNA samples of family members were isolated from peripheral blood lymphocytes, and whole exome sequencing (WES) was performed on a HiSeq XTen Deep Sequencer (Illumina, CA, USA), with an average coverage of ~36X, according to the manufacturer's instructions. The primary data analysis was done by a combination of Burrows-Wheeler Alignment (BWA) sequence aligner for reads alignment to human reference genome GRCh37/hg19, Genome Analysis Toolkit (GATK) pipeline for calling single-nucleotide variant (SNV), and small insertion and deletion (indel), and ANNOVAR for variant characterization ¹⁸⁻²⁰. Identified variants were filtered through comparison with the disease-associated variants in the known databases (Human Gene Mutation Database (HGMD, 2020.2) and the Online Mendelian Inheritance in Man (OMIM)) and polymorphism databases (dbSNP143, 1000 Genome). Sanger sequencing of the CRMP1 gene (NM 001014809) was performed to confirm the identified variants in the patients and further family members and performed segregation analysis of the variants with the phenotype. In family 2, variants were detected by routine WES diagnostics and variant calling using a parent-offspring trio approach as described previously ²¹. Briefly, the exome was captured using the Agilent SureSelectXT Human All Exon v5 library prep kit (Agilent Technologies,

122

123

124

125

126

127

128

129

130

131

132

133

134

135

136

137

138

139

140

141

142

143

144

145

Santa Clara, CA, USA). Exome libraries were sequenced on an Illumina HiSeq 4000 instrument (Illumina, San Diego, CA, USA) with 101 bp paired-end reads at a median coverage of 75× at the BGI Europe facilities (BGI, Copenhagen, Denmark). Sequence reads were aligned to the hg19 reference genome using Burrows-Wheeler Alignment (BWA) and variants were subsequently called by the Genome Analysis Toolkit (GATK) unified genotyper, version 3.2-2 and annotated using a custom built diagnostic annotation pipeline. Multi-species sequence alignment were performed using Multialin, PhyloP and PhastCons and the variants disease- causative nature were predicted using the free online tool Mutation Taster (www.mutationtaster.org). In family 3, trio-based whole-genome sequencing was performed on blood-derived genomic DNA at the Laboratoire de biologie médicale multisites SeqOIA (LBMS SeqOIA, Paris, France). After extraction, DNA samples were sonicated, and libraries were prepared using the NEBNext Ultra-II kit (New England Biolabs). Whole-genome sequencing was performed in paired-end 2x150-bp mode, with a NovaSeq6000 (Illumina). Demultiplexed data were aligned to the genomic reference (hg19). Recalibration and variant calling was performed using GATK4 (Broad Institute). Short variants were annotated with SNPeff (4.3t). Copy Number Variants >4kb were called using CNVnator (v0.4.1) and annotated with AnnotSV (v2.5.1). An average depth-of-coverage of >50x was obtained for both probands, and variants were prioritized according to impact, frequency, and segregation. Sanger sequencing was performed to confirm the identified mutation in the CRMP1 gene. Expression and purification of recombinant hCRMP1 variants. Subcloned GST-tagged CRMP1B-V5 expression plasmids (wildtype, P475L, T313M) were transformed into E. coli BL21 (DE3) pLysS cells (BioDynamics Laboratory, Tokyo, Japan). These bacteria were harvested to 200 ml Terrific Broth medium (Invitrogen, Waltham, MA, USA) including 100 mg/ml ampicillin (Sigma, St. Louis, MO, USA). After incubation for 1.5 h at 37 °C, the

147

148

149

150

151

152

153

154

155

156

157

158

159

160

161

162

163

164

165

166

167

168

169

170

protein production was induced by 0.1 mM isopropyl β-D-1-thiogalactopyranoside (Sigma) for 18 h at 20 °C. Collected bacteria by centrifugation were suspended in 24 ml homogenization buffer (H buffer; 50 mM Tris/HCl (pH 8.0), 100 mM KCl, 1 mM EDTA, 5% glycerol, 1% NP-40, 1 mM DTT) and then sonicated 4 times for 5 min on ice using Ultrasonic Homogenizer (Microtec Co., LTD., Chiba, Japan). After centrifugation at 12,000 rpm for 30 min at 4 °C, resultant supernatants were mixed with 400 µl of Glutathione Sepharose 4FF resin (Cytiva, Tokyo, Japan) and gently inverted for 24 h at 4 °C. The resins were collected and washed 4 times with 10 ml H buffer, and then washed 5 times with 1 ml cleavage buffer (C buffer; 20 mM Tris/HCl (pH 8.0), 150 mM NaCl, 0.1% NP-40, 1 mM DTT). The pelleted resins were suspended in 100 µl of C buffer including 10 U PreScission protease (Cytiva) and incubated for 24 h at 4 °C with constant agitation. These mixtures were transferred to the filter cups (Vivaclear Mini 0.8 µm PES; Sartorius, Stonehouse, UK), and the flow through fractions were obtained by centrifugation at 10,000 rpm for 1 min at 4 °C. Protein concentrations were determined using the Bradford reagent (Thermofisher scientific, Waltham, MA, USA), and the purified mutants were assessed by SDS-PAGE. Determination of dominant-negative effect of the CRMP1 variants on the multimer formation of the wild type. HEK293T cells were co-transfected with pc3.1beta2-V5-CRMP1B-wildtype and either one of myc-tagged CRMP1B constructs (wildtype, P475L or T313M). After 24h incubation, the cells were harvested by modified C buffer (20 mM Tris/HCl (pH 8.0), 150 mM NaCl, 1% NP-40, 1 mM DTT, protease inhibitor cocktail (cOmplete mini; Roche)), sonicated for 15 min, and centrifuged at 15,000 rpm for 30 min at 4 °C. Electrophoresis of the resultant supernatants under the native and denaturing state were performed as described above. Semi-dry Western transfers were carried out at 15 V for 60 min using the transfer buffer, 50 mM Tris, 40 mM glycine, 20% methanol, 0.1% SDS. In the case of the BN-PAGE, the transferred membranes were incubated in 8% acetic acid for 15

172

173

174

175

176

177

178

179

180

181

182

183

184

185

186

187

188

189

190

191

192

193

194

195

min, washed by ultrapure water, and then dried completely, followed by decolorization using 100% methanol. After blocking by 5% skim milk in TBS-T (20 mM Tris/HCl (pH 7.4), 150 mM NaCl, 0.1% Tween-20) for 60 min, the membranes were reacted with anti-myc (9E10) mAb (1:2,000, FUJIFILM, Cat No. 011-21874) or anti-V5 mAb (1:10,000, Invitrogen (R960–25) RRID: AB_2556564) for overnight at 4 °C. Infrared-fluorescence- (IRDye 680RT; LI-COR, Lincoln, NE, USA) or HRP-conjugated (Dako, Santa Clara, CA, USA) secondary antibodies were utilized for the detection of the first antibodies on the membranes obtained from the native or denatured electrophoresis, respectively. Transfection to primary cultured mouse embryonic cortical neurons. Pregnant ICR (RRID:IMSR TAC:icr) female mice were purchased from Nihon SLC (Shizuoka, Japan). Overdose isoflurane (7 - 8%)/air mixture was inhaled to euthanize the pregnant ICR mice until the loss of breathing. The E15-16 mouse embryos dissected from the pregnant mice were immediately placed in ice-cold PBS and euthanized by decapitation. Cortices dissected from the embryos were treated with 1% trypsin/PBS at 37 °C for 5 min and quenched with the addition of 0.5% trypsin inhibitor. The dissociated neurons were centrifuged at 800 xg for 5 min at 4 °C, washed once, and suspended in DMEM-10% FBS. The cells (1.0×10^6) were transfected with 10 µg of pc3.1beta2-V5 harboring CRMP1B-wildtype, -P475L, or -T313M or using an electroporation equipment NEPA21 (NEPA GENE, Chiba, Japan). The condition of electroporation was follows: Poring pulse (275 V, 0.5 ms pulse length, 50 ms pulse interval, 10% decay, +pulse orientation, 2 times); Transfer pulse (20 V, 50 ms pulse length, 50 ms pulse interval, 40% decay, ±pulse orientation, 5 times). The cells were suspended in DMEM-10% FCS and seeded (1 \times 10⁴/well) on a 24 well culture-plate coated with 0.05 mg/ml of poly-l-lysine (Wako, Cat No. 163-19091). After overnight incubation, the medium was replaced with Neurobasal medium supplemented with 2% B-27, 2 mM Glutamax, 50 U/ml penicillin, and 50 μg/ml streptomycin (500 μl/well) and incubated 37 °C for 6–7 days.

197

198

199

200

201

202

203

204

205

206

207

208

209

210

211

212

213

214

215

Immunocytochemistry of mice cortical cultured neurons. The primary cultured cortical neurons were fixed with 4% paraformaldehyde (PFA)/PBS for 30 min at 25 °C, replaced with PBS, and stored at 4 °C. As the expression of V5-CRMP1B constructs was limited, tyramide signal amplification (TSA) system (PerkinElmer, Cat No. NEL700A001KT) was applied for the detection of V5 signal. Briefly, the cells were treated with PBS containing 0.3% H₂O₂ for 20 min at 25 °C and blocked with 1:1 mixture of PBS supplemented with 0.1% Triton X-100 (PBST) containing 10% skim milk and Tris-buffered serine supplemented with 0.1% Triton X-100 (TBST) containing 5% normal goat serum (NGS) for 30 min at 25 °C. The cells were washed twice with TBST and incubated with the primary antibody mixture consisting of TBST 2.5% NGS, anti-V5 mouse mAb (1:5000) and anti-MAP2 rabbit pAb (1:5000, Covance (PRB-547C) RRID: AB_2565455) for overnight at 4 °C. The cells were sequentially incubated each for 1h at 25°C with TBST 2.5% NGS containing biotin-conjugated anti-mouse secondary antibody (1:3000, Jackson) and TBST 2.5% NGS containing streptavidin-HRP conjugate (1/500, dilution, PerkinElmer). Then the cells were reacted with tyramide signal amplification mixture for 10min at 25°C and subsequently incubated with TBST 2.5% NGS containing streptavidin-Alexa594 (1:2000) and anti-rabbit secondary antibody-Alexa488 for 2 h at 25 °C. The images of immunostained neurons were captured by an Olympus IX70 microscope equipped with x10 Objective lens and DP74 camera. The neurite outgrowth of V5- or tdTomato- positive neurons was scored with Fiji software (2.0.0-rc-59/1.51n). In each condition, 13 to 20 V5- or tdTomato-positive neurons were analyzed.

Results

216

217

218

219

220

221

222

223

224

225

226

227

228

229

230

231

232

233

234

235

236

237

238

239

240

241

Phenotype and genotype of index patients

Proband 1 (P1) was born as the second child of non-consanguineous healthy parents of Caucasian descent after an uneventful pregnancy (Fig 1A, Table 1). At delivery a singular umbilical artery was noted. The global development was delayed from infancy on: with sitting at 1.5-2 years-of-age, standing with support at 1-1.5 years-of-age, walking at 2-2.5 years-ofage, first words at 2-2.5 years-of-age. Standardized cognitive tests performed at 5-10 years revealed a moderate intellectual disability with an intelligence quotient (IQ) of 55 at last assessment using the Kaufman Assessment battery for children (K-ABC). She had speech disorder. Behavioral problems included a lack of distance to men and a sexualized behavior. At last assessment at 15-16 years-of-age, the girl had generalized muscular hypotonia with normal reflexes, but fine motor problems with a broad-based gait but no ataxia. When climbing stairs, she showed clear instability. The results of cranial magnetic resonance imaging (MRI) at 1.5 - 4 years as well as that of further work-up (including metabolic tests, electroencephalogram (EEG). ophthalmological assessment, electrocardiogramm, echocardiogramm, abdominal sonography) were normal. Since preliminary genetic tests including chromosome analysis and array-CGH were normal in the index patient (P1), we performed whole exome sequencing (WES) to identify the underlying genetic cause. WES followed by bioinformatic analysis and confirmation with Sanger sequencing revealed the heterozygous de novo variant in the CRMP1 gene c.1766C>T (NM_001014809.2; Chr4 (GRCh37):g.5830253G>A) in the affected child P1 (**Fig 1B**). At the protein level, this variant leads to an amino acid change at position 589 from proline to leucine: P589L in long isoform, CRMP1A (NP_001014809.1) and P475L in short form, CRMP1B (NP_001304.1) (Fig 1B). The identified variant was not found in 1000Genomes, dbSNP or gnomAD. The CADD score (https://cadd.gs.washington.edu/) was 24.5. The mutation localizes to a highly conserved position, as demonstrated by PhyloP (5.327), PhastCons (1) score and multi-species sequence

243

244

245

246

247

248

249

250

251

252

253

254

255

256

257

258

259

260

261

262

263

264

265

266

267

alignment (Fig 1C). The Provean score of the identified variants predicted to have a deleterious effect (-5.854, cutoff= -2.5). Proband 2 (P2) was born as the second child of non-consanguineous parents of Caucasian descent after an uneventful pregnancy and delivery (Fig 1A, Table 1). The boy was macrosomic at birth but had no congenital microcephaly. His motor development was delayed (unsupported walking at 2-2.5 years-of-age) due to congenital mild muscular hypotonia with normal deep tendon reflexes, but no coordination problems. He had bilateral pes planus. A speech delay and language impairment with first words spoken at 3-3.5 years-of-age were diagnosed. He was also diagnosed with an autism spectrum disorder and normal cognitive abilities (IQ 95). At last assessment at 10-11 years-of-age, an obesity associated with hyperphagia was of raising concern, and he had secondary enuresis nocturna. The results of a cranial MRI and EEG were normal. Similarly, through WES followed by bioinformatic analysis, we identified a heterozygous de novo variant c.1280C>T in the CRMP1 gene (NM_001014809.2; Chr4 (GRCh37):g.5841279G>A) in proband (P2) (**Fig 1B**). This variant leads to an exchange of threonine to methionine at position 427 in the long form, CRMP1A (p.T427M, NP 001014809.1) and at position 313 in the short form, CRMP1B (p.T313M, NP_001304.1) (Fig 1B). The variant affects a highly conserved region of the protein (Fig 1C). Proband 3 (P3) is the first child of three of a non-consanguineous family of European descent (Fig 1A, Table 1). She was born at gestation week 40 after an uneventful pregnancy, with normal birth parameters (weight: 3.610 kg, height: 50 cm, head circumference: 32.5cm, Apgar score: 10/10). She had developmental delay with not being able to sit alone at 1-1.5 years-of-age and walked without support at 2-2.5 years-of-age. Her speech development was delayed with few words spoken at 2.5-3 years-of-age. She began to gain weight from 1.5-2 years-of-age, and overgrowth was noticed since the 2-2.5 years-of-age. Endocrinological screening, including leptin blood level was normal. There is familial history of obesity on

269

270

271

272

273

274

275

276

277

278

279

280

281

282

283

284

285

286

287

288

289

290

291

292

both parental sides, and one of the parent is macrocephalic. She developed severe behavioral issues with temper tantrums, stubbornness, hyperphagia, obsessive-compulsive characteristics and autism spectrum disorder. She was attending medical-educational institute at the age of 8-8.5 years. At the last assessment of 13-14 years-of-age, she had moderate intellectual disability and persistent severe behavioral disorders. Distinctive facial features were low forehead hair insertion, anteverted and large earlobes, broad nasal tip, short philtrum and full lower lips. Genu valgum and hyperlordosis as well as abdominal and dorsal strech marks were noted. Enuresia was noted. Cerebral MRI and abdomino-renal ultrasound were normal. Metabolics and storage disease screening were negative. Array analysis revealed two maternally inherited deletions: a 668 kb deletion at 3q26.31 and a 371kb at 5q23.1, confirmed by genome sequencing and considered as variant of unknown significance. Further analysis through trio-based whole-genome sequencing identified a de novo variant in the CRMP1 gene c.1052T>C (NM_001014809.2; Chr4 (GRCh37):g.5841409A>G) (Fig 1B). The identified variant leads to an exchange of phenyl alanine to serine at position 351 of long form of CRMP1 (CRMP1A (NP_001014809.1)) and at position 237 in short form (CRMP1B (NP 001304.1)) and it is located in the highly conserved region of the protein (**Fig 1C**). This variant is not found in gnomAD database. In silico pathogenicity prediction tools predicts the identified variants to be deleterious (CADD pared: 23.60; REVEL 0.577 (Thresholds > 0.5 Damaging), ClinPred 0.975 (Damaging \geq 0.5), Mistic: 0.90 (Damaging Threshold \geq 0.5)). No additional pathogenic variants have been identified by trio genome sequencing, including all known genes involved in neurodevelopmental disorder.

Effect of identified CRMP1 variants on protein structure

Since CRMP1 is known to oligomerize to form homotetramers and heterotetramers along with other CRMPs to regulate cellular functions, we determined the effect of the identified human variants on its protein structure using known structures and protein structure prediction

294

295

296

297

298

299

300

301

302

303

304

305

306

307

308

309

310

311

312

313

314

315

316

317

tools. The structure of CRMP1 short form, CRMP1B, has been determined at 3.05A resolution²² lacking the N-terminal 14 residues and residues 491-572 in their C-terminal region. CRMP1 monomer consists of three structural parts, N-terminal β-strands followed by a linker β -strand connected to the central α/β -barrel (**Fig 1D**). Several residues contribute to the oligomerization interface of CRMP1 and the quaternary structure of CRMP1 tetramer is shown in Fig 1E. The amino acid exchange of P475L, T313M, and F237S are located in the highly conserved region of CRMP1. The P475L is the last residue before the start of the Cterminal helix and the exchange of proline to leucine is predicted to lead to serious clashes with the neighboring residues (Fig 1F). Such spatial constraints may alter the dipole moment of the helix and lead to long-range allosteric effects (Fig 1G). The T313M lies within the region of the α/β -barrel, is oriented towards the inside of the protein and located close to the ligand-binding active site/cavities (Fig 1H). Rearrangements within the protein upon interaction with other CRMPs or molecules could shuffle these cavities for normal functioning. The exchange of threonine to methionine is predicted to prevent rearrangements and to affect the oligomerization as well as other interactions. The F237S is localized directly in the center of interface 1 so the exchange of a heavy hydrophobic sidechain by a hydrophilic short sidechain most likely interferes with the stability of the dimer interaction (Fig 11). Based on structural simulations, all three variants are predicted to affect the ternary structure of CRMP1 and impact on its oligomerization.

P475L and T313M mutations affect homo-oligomerization of CRMP1B

To analyze the effect of *CRMP1* variants on its protein levels and cellular function, two variants (CRMP1B-P475L (P1) or -T313M (P2)) were chosen for further functional analysis. We purified the recombinant human CRMP1B-wildtype, -P475L (P1) or -T313M (P2) proteins using the *E. coli* GST-tag expression system. CRMP1B-wildtype showed two major 64 kDa and 60 kDa bands on SDS-denatured gel electrophoresis (**Fig 2A, left lane**). The 64

319

320

321

322

323

324

325

326

327

328

329

330

331

332

333

334

335

336

337

338

339

340

341

342

kDa and 60 kDa correspond to full-length CRMP1B and to a truncated, C-terminal region cleaved form, respectively. The yield of purified T313M (TM) or P475L (PL) was less than that of wildtype in the same condition (Fig 2A, middle and right lanes). This finding may be due to lower expression and/or aggregation of the mutant proteins in E. coli. As T313M and P475L mutated residues are positioned close to the dimer/tetramer interface of CRMP1B, these mutations may affect homo-oligomerization of CRMP1. We therefore examined the oliogomerization of recombinant CRMP1 preparation with Blue-Native gel electrophoresis (Fig 2B). A broad band of CRMP1B-wildtype was present at high (720 kDa) but residual amount of monomeric form was detected at low molecular weight (70 kDa) on Blue-Native gel. The 720 kDa band probably represents the homo-oligomerization of CRMP1B-wildtype under the native condition. In contrast, CRMP1B-T313M and -P475L showed the increased monomeric 70 kDa band, suggesting weakened self-association of these mutants. As these mutations were found in the heterozygous state in the affected patients, CRMP1B-T313M and/or -P475L expression might perturb the oligomerization of CRMP1B-wildtype in a dominant-negative manner. We therefore next co-expressed V5-CRMP1B-wildtype together with either myc-CRMP1B-wildtype, -T313M, or -P475L in HEK293T cells. As shown in Fig **2C** upper and middle panels, co-expression of myc-CRMP1B-T313M or -P475L did not alter the expression level of V5-CRMP1B-wildtype on SDS-denatured gel electrophoresis. Anti-V5 immunoblot analysis of these specimens on Blue-Native gel electrophoresis (Fig 2C, lower panel) revealed that the co-expression of myc-CRMP1B-wildtype showed major 1100 kDa and minor 360 kDa bands of V5-CRMP1-wildtype. In contrast, co-expression of myc-CRMP1B-T313M or -P475L increased the lower (360 kDa) V5-CRMP1B-wildtype, suggesting that these mutants potentially impede multimer formation of CRMP1B-wildtype. As V5-immunoreactive signal at higher molecular size (1100 kDa) in P475L was remarkably decreased than that in T313M, P475L may exhibit stronger dominant negative effect.

P475L and T313M mutations attenuate neurite outgrowth of cortical neurons

We next asked whether the ectopic expression of *CRMP1B* mutants in primary cultured murine cortical neurons affect the neuronal development. Dissociated E15 mouse cortical neurons were electroporated with the expression vector harboring either V5-*CRMP1B*-wildtype (wt), -T313M (TM), -P475L (PL), or tdTomato. The cells were seeded onto PLL-coated culture dishes and grown for 6-7 days. After fixation, the cells were immunostained with anti-V5 and anti-MAP2 antibodies. We found that the longest primary neurites of V5-*CRMP1B*-T313M or -P475L transfected neurons were shorter than those of V5-*CRMP1B*-wildtype (wt) or tdTomato transfected cells (**Fig 3A-D**). We then measured the length of the longest primary neurite from V5- or tdTomato-positive neurons in each condition. The longest primary neurites expressing *CRMP1B*-T313M or -P475L were 40-50% shorter than those expressing *CRMP1B*-wildtype (wt) (**Fig 3E**). As the longest primary neurites of the cultured cortical neurons is thought to be axons, these *CRMP1B* mutants may interfere with the oligomerization of *CRMP1* in turn to attenuate the outgrowth of the cortical axons.

Discussion

357

358

359

360

361

362

363

364

365

366

367

368

369

370

371

372

373

374

375

376

377

378

379

380

381

382

In this study, we report the human phenotype associated with heterozygous CRMP1 variants in three affected children of unrelated non-consanguineous pedigrees. All the patients have a neurodevelopmental disorder with motor delay and muscular hypotonia. While patient P1 has moderate intellectual disability and behavioral abnormalities, P2 was diagnosed with an autism spectrum disorder but a normal cognitive profile and P3 presented with moderate intellectual disability and autism spectrum disorder. We showed that those human CRMP1 variants have a dominant-negative effect and impact the oligomerization of CRMP1 proteins. CRMP1 exists as homo- or hetero-tetramers to interact with various signaling molecules and to link microtubules to subcellular structures and regulate cytoskeletal dynamics.^{5,23} In line with this, CRMP1 colocalizes to the mitotic spindles and centrosomes, indicating of playing a key role in mitosis and cell cycle progression.²⁴ Defective cell cycle, abnormal mitotic spindle and centrosomes are the common key pathomechanism underlying several neurodevelopmental disorders.²⁵ Dysregulation of other CRMPs that have been linked to human disease has been shown to affect specific cellular processes associated with the clinical phenotype. For example, mutant CRMP5 impedes the ternary complex formation with microtubule-associated protein 2 (MAP2) and beta-III-tubulin, thereby causing a defective inhibitory regulation on neurite outgrowth and dendritic development and thereby contribute to the brain malformation phenotype. 13 MAP2 has been already reported to play a key role in neurite outgrowth and synaptic plasticity through its role in microtubule stabilization and cytoskeletal association. 26,27 Also, mutant CRMP4 was shown to affect axonal growth and survival of motor neurons and thereby contribute to the amyotrophic lateral sclerosis phenotype. ¹⁴ In this study we showed that the identified CRMP1 variants affect neurite outgrowth, which is a characteristic phenotype associated to many neurodevelopmental/psychiatric disorders. ²⁸ Our finding is in line with the reduced neurite outgrowth phenotype and impaired long-term

384

385

386

387

388

389

390

391

392

393

394

395

396

397

398

399

400

potentiation in the Crmp1^{-/-} mice. Mechanistically, these cellular processes are regulated in a spatiotemporal manner through CRMP1 phosphorylation by several kinases such as Cdk5, Rho/ROCK or GSK3, and any disturbances in these kinases or mutation of specific residues culminates in the abnormal brain development.^{6,8-11,29} In the case of *Cdk5*^{-/-} mice, abnormal dendritic spine morphology was shown in cortical neurons as it was in Crmp1^{-/-} mice. Intriguingly, both mouse models show schizophrenia-like behavior, indicating the commonly shared cellular mechanism for dendritic development. 9,30 In the context of neuronal development, defective phosphorylation of tyrosine residues in CRMP1 by Fyn-mediated Reelin signaling impairs cortical neuron migration.⁶ Over the last two decades, new phosphorylation specific sites in CRMP1 are being reported and recently, phosphorylation of Tyr504 residue by Fyn has been shown to play an important step in Sema3A-regulated dendritic development of cortical neurons.³¹ As a future perspective, it will be interesting to find other CRMP1 variants and elucidate the role of specific residues in various neuronal process and associate with the phenotypic spectrum of neurodevelopmental disorder. In conclusion, we report for the first time human CRMP1 mutations, link them to a human neurodevelopmental disease and highlight underlying pathomechanisms. Our report adds CRMP1 to list of other CRMP genes linked to neurological disorders and underlines the important role of CRMP1 in the nervous system development and function.

Declaration of interest

The authors declare no competing interests.

Data availability

- 405 All methods applied in this project are described in detail in the 'Materials and
- 406 Methods's ection and the original data are presented as source file

Acknowledgements

The authors thank the index families for their participation in this study. We acknowledge Petra Bittigau, Akosua Sarpong for attending the patients; Anna Tietze for the analysis of cranial MR images; Sabrina Pommer and Jessica Fassbender for technical assistance; Piotr Neumann for assistance in data interpretation and lively discussions; Dr. Tanabe Kenji and Dr. Fumitoshi Saitoh for electroporation equipment. We acknowledge the funding resources for this study: German Research Foundation (SFB665, SFB1315, FOR3004, AMK), the Sonnenfeld Stiftung (AMK, KLM), the Berlin Institute of Health (BIH, CRG1, AMK), the Charité (AMK, ER, LLB, KLM), and by grants-in-aid for Scientific Research from the Japan Society for the Promotion of Science (JSPS) (16K07062) (FN).

References

418

- 1. Rice D, Barone S, Jr. Critical periods of vulnerability for the developing nervous
- system: evidence from humans and animal models. Environ Health Perspect. Jun 2000;108
- 421 Suppl 3:511-33. doi:10.1289/ehp.00108s3511
- 422 2. Gilbert SL, Dobyns WB, Lahn BT. Genetic links between brain development and
- 423 brain evolution. *Nat Rev Genet*. Jul 2005;6(7):581-590. doi:10.1038/nrg1634
- 424 3. Strittmatter L-HWaSM. A Family of Rat CRMP Genes Is Differentially Expressed in
- 425 the Nervous System. *J Neurosci* 1996;16:6197–6207
- 426 4. Bretin S, Reibel S, Charrier E, et al. Differential expression of CRMP1, CRMP2A,
- 427 CRMP2B, and CRMP5 in axons or dendrites of distinct neurons in the mouse brain. J Comp
- 428 Neurol. May 23 2005;486(1):1-17. doi:10.1002/cne.20465
- 429 5. Wang LH, Strittmatter SM. Brain CRMP forms heterotetramers similar to liver
- 430 dihydropyrimidinase. *J Neurochem*. Dec 1997;69(6):2261-9. doi:10.1046/j.1471-
- 431 4159.1997.69062261.x
- 432 6. Yamashita N, Uchida Y, Ohshima T, et al. Collapsin response mediator protein 1
- 433 mediates reelin signaling in cortical neuronal migration. J Neurosci. Dec 20
- 434 2006;26(51):13357-62. doi:10.1523/JNEUROSCI.4276-06.2006
- 435 7. Naoya Yamashita AM, Yutaka Uchida, Fumio Nakamura, Hiroshi Usui, Toshio
- 436 Ohshima, Masahiko Taniguchi, Jérôme Honnorat, Nicole Thomasset, Kohtaro Takei, Takuya
- 437 Takahashi, Pappachan Kolattukudy, Yoshio Goshima. Regulation of spine development by
- 438 semaphorin3A through cyclin-dependent kinase 5 phosphorylation of collapsin response
- 439 mediator protein 1. *J Neurosci*
- 440 2007 (Nov 14;27(46):12546-54)
- 441 8. Hiroko Makihara SN, Wataru Ohkubo, Naoya Yamashita, Fumio Nakamura, Hiroshi
- 442 Kiyonari , Go Shioi , Aoi Jitsuki-Takahashi , Haruko Nakamura, Fumiaki Tanaka , Tomoko
- 443 Akase, Pappachan Kolattukudy, Yoshio Goshima CRMP1 and CRMP2 have synergistic but
- distinct roles in dendritic development. *Genes Cells*. 2016;Sep;21(9):994-1005.
- 445 9. Su KY, Chien WL, Fu WM, et al. Mice deficient in collapsin response mediator
- 446 protein-1 exhibit impaired long-term potentiation and impaired spatial learning and memory.
- 447 *J Neurosci*. Mar 7 2007;27(10):2513-24. doi:10.1523/JNEUROSCI.4497-06.2007
- 448 10. Charrier E, Mosinger B, Meissirel C, et al. Transient alterations in granule cell
- proliferation, apoptosis and migration in postnatal developing cerebellum of CRMP1-/- mice.
- 450 Genes Cells. Dec 2006;11(12):1337-52. doi:10.1111/j.1365-2443.2006.01024.x
- 451 11. Yutaka Uchida TO, Yukio Sasaki, Hiromi Suzuki, Shigeki Yanai, Naoya
- 452 Yamashita, Fumio Nakamura, Kohtaro Takei, Yasuo Ihara, Katsuhiko Mikoshiba, Papachan
- Kolattukudy, Jerome Honnorat, Yoshio Goshima. Semaphorin 3A signalling is mediated via
- 454 sequential Cdk5 and GSK3β phosphorylation of CRMP2: implication of common
- 455 phosphorylating mechanism underlying axon guidance and Alzheimer's disease. Genes to
- 456 *Cells* 2005;(10,165–179)
- 457 12. Yoshimura T, Kawano Y, Arimura N, et al. GSK-3beta regulates phosphorylation of
- 458 CRMP-2 and neuronal polarity. *Cell*. Jan 14 2005;120(1):137-49.
- 459 doi:10.1016/j.cell.2004.11.012
- 460 13. Jeanne M, Demory H, Moutal A, et al. Missense variants in DPYSL5 cause a
- 461 neurodevelopmental disorder with corpus callosum agenesis and cerebellar abnormalities. Am
- 462 J Hum Genet. May 6 2021;108(5):951-961. doi:10.1016/j.ajhg.2021.04.004
- 463 14. Blasco H, Bernard-Marissal N, Vourc'h P, et al. A rare motor neuron deleterious
- 464 missense mutation in the DPYSL3 (CRMP4) gene is associated with ALS. *Hum Mutat*. Jul
- 465 2013;34(7):953-60. doi:10.1002/humu.22329

- 466 15. Braunschweig D, Krakowiak P, Duncanson P, et al. Autism-specific maternal
- 467 autoantibodies recognize critical proteins in developing brain. Transl Psychiatry. Jul 9
- 468 2013;3:e277. doi:10.1038/tp.2013.50
- 469 16. Bader V, Tomppo L, Trossbach SV, et al. Proteomic, genomic and translational
- approaches identify CRMP1 for a role in schizophrenia and its underlying traits. Hum Mol
- 471 *Genet.* Oct 15 2012;21(20):4406-18. doi:10.1093/hmg/dds273
- 472 17. Naoya Yamashita AT, Keizo Takao, Toshifumi Yamamoto, Pappachan Kolattukudy,
- 473 Tsuyoshi Miyakawa, Yoshio Goshima. Mice lacking collapsin response mediator protein 1
- 474 manifest hyperactivity, impaired learning and memory, and impaired prepulse inhibition.
- 475 *Front Behav Neurosci.* 2013 (Dec 27;7:216.)
- 476 18. Li H, Durbin R. Fast and accurate long-read alignment with Burrows-Wheeler
- 477 transform. *Bioinformatics*. Mar 1 2010;26(5):589-95. doi:10.1093/bioinformatics/btp698
- 478 19. Wang K, Li M, Hakonarson H. ANNOVAR: functional annotation of genetic variants
- 479 from high-throughput sequencing data. *Nucleic Acids Res.* Sep 2010;38(16):e164.
- 480 doi:10.1093/nar/gkq603
- 481 20. Mark A DePristo EB, Ryan Poplin, Kiran V Garimella, Jared R Maguire, Christopher
- 482 Hartl, Anthony A Philippakis, Guillermo del Angel, Manuel A Rivas, Matt Hanna, Aaron
- 483 McKenna, Tim J Fennell, Andrew M Kernytsky, Andrey Y Sivachenko, Kristian Cibulskis,
- 484 Stacey B Gabriel, David Altshuler & Mark J Daly A framework for variation discovery and
- genotyping using next-generation DNA sequencing data. Nature Genetics. 2011;(43,
- 486 pages491–498 (2011))
- 487 21. de Ligt J, Willemsen MH, van Bon BW, et al. Diagnostic exome sequencing in
- persons with severe intellectual disability. N Engl J Med. Nov 15 2012;367(20):1921-9.
- 489 doi:10.1056/NEJMoa1206524
- 490 22. Liu SH, Huang SF, Hsu YL, et al. Structure of human collapsin response mediator
- 491 protein 1: a possible role of its C-terminal tail. Acta Crystallogr F Struct Biol Commun. Aug
- 492 2015;71(Pt 8):938-45. doi:10.1107/S2053230X15009243
- 493 23. Nakamura F, Kumeta K, Hida T, et al. Amino- and carboxyl-terminal domains of
- 494 Filamin-A interact with CRMP1 to mediate Sema3A signalling. Nat Commun. Oct 31
- 495 2014;5:5325. doi:10.1038/ncomms6325
- 496 24. Shih JY, Lee YC, Yang SC, et al. Collapsin response mediator protein-1: a novel
- 497 invasion-suppressor gene. Clin Exp Metastasis. 2003;20(1):69-76.
- 498 doi:10.1023/a:1022598604565
- 499 25. Zaqout S, Kaindl AM. Autosomal Recessive Primary Microcephaly: Not Just a Small
- 500 Brain. Front Cell Dev Biol. 2021;9:784700. doi:10.3389/fcell.2021.784700
- 501 26. Kaech S, Parmar H, Roelandse M, Bornmann C, Matus A. Cytoskeletal
- 502 microdifferentiation: a mechanism for organizing morphological plasticity in dendrites. *Proc*
- 503 Natl Acad Sci U S A. Jun 19 2001;98(13):7086-92. doi:10.1073/pnas.111146798
- 504 27. Sanchez C, Diaz-Nido J, Avila J. Phosphorylation of microtubule-associated protein 2
- 505 (MAP2) and its relevance for the regulation of the neuronal cytoskeleton function. Prog
- 506 Neurobiol. Jun 2000;61(2):133-68. doi:10.1016/s0301-0082(99)00046-5
- 507 28. Prem S, Millonig JH, DiCicco-Bloom E. Dysregulation of Neurite Outgrowth and Cell
- 508 Migration in Autism and Other Neurodevelopmental Disorders. Adv Neurobiol. 2020;25:109-
- 509 153. doi:10.1007/978-3-030-45493-7_5
- 510 29. Yamashita N, Goshima Y. Collapsin response mediator proteins regulate neuronal
- 511 development and plasticity by switching their phosphorylation status. *Mol Neurobiol*. Apr
- 512 2012;45(2):234-46. doi:10.1007/s12035-012-8242-4
- 513 30. Yamashita N, Takahashi A, Takao K, et al. Mice lacking collapsin response mediator
- 514 protein 1 manifest hyperactivity, impaired learning and memory, and impaired prepulse
- 515 inhibition. Front Behav Neurosci. 2013;7:216. doi:10.3389/fnbeh.2013.00216

- 516 31. Kawashima T, Jitsuki-Takahashi A, Takizawa K, et al. Phosphorylation of Collapsin
- Response Mediator Protein 1 (CRMP1) at Tyrosine 504 residue regulates Semaphorin 3A-
- 518 induced cortical dendritic growth. *J Neurochem*. May 2021;157(4):1207-1221.
- 519 doi:10.1111/jnc.15304

Table 1: Phenotype of patients with CRMP1 variants.

520521

Characteristics and Symptoms	Proband 1 (Pedigree 1)	Proband 2 (Pedigree I1)	Proband 3 (Pedigree I1I)
CRMP1 variant	. 1766С\ Т.	a 1000Cs Ts	a 1050T\ C.
(NM_001014809.2);	c.1766C>T;	c.1280C>T;	c.1052T>C;
(NP_001014809.1)	p.P589L	p.T427M	p.F351S
Parents	non- consanguineous	non- consanguineous	non- consanguineous
Gender	female	male	female
Anthropometric data	normal	normal	Overgrowth
weight (kg)	57.1 (0.15 SD)	N/A	133 (14.2 SD)
height (cm)	168 (0.43 SD)	1,711	166.5 (2.94 SD)
OFC (cm)	53.5 (-1.02 SD)		62 (5 SD)
Pregnancy, birth, postnatal	(1.02 02)		02 (0 00)
adaption	normal	normal	normal
singular umbilical artery	+	-	-
macrosomia	_	+	_
fetal fingerpads	_	+	_
Microcephaly (OFC < -2 SD)	-	-	_
Macrocephaly (OFC >-2 SD)	-	-	+ (5 SD)
Facial dysmorphism	-	-	+
Delayed motor development	+	+	+
walking unsupported (years)	2-2.5	2-2.5	2-2.5
Global muscular hypotonia	mild	mild	mild
Deep tendon reflexes	normal	normal	normal
Intellectual disability	moderate (IQ 55)	no (IQ 95)	moderate
Autism spectrum disorder	-	+	-
Behavioral problems			
lack of distance, sexualized	+	+	+
behavior	+	-	-
hyperphagia	-	+	+
Delayed speech and language			
development	+	+	+
(first words spoken) (years)	(2-2.5)	(3-3.5)	(3-3.5)
Fine motor problems	+	-	+
Other			
secondary enuresis			
nocturna	-	+	+
pes planus	-	+	-
obesity	-	+	+
EEG results	normal	normal	normal
Cranial MRI abnormalities	-	-	-

^{+,} yes; -, no; IQ, intellectual quotient; N/A, not available; OFC, occipitofrontal circumference; SD, standard deviation

Figure Legends:

524

525

526

527

528

529

530

531

532

533

534

535

536

537

538

539

540

541

542

543

544

545

546

547

Fig 1: Genotype of patients with variants in CRMP1. A. Pedigree of index families. B. Pictogram representing the CRMP1 cDNA with identified variant of proband 1 (P1) in exon 12 (c.1766C>T, NM_001014809.2) which leads on protein level to an amino acid change of proline to leucine in CRMP1 (CRMP1A-long form (p.P589L, NP_001014809.1) and CRMP1B-short form (p.P475L, NP 001304.1)); the variant in proband 2 (P2) in exon 9 c.1280C>T (NM_001014809.2) leads to an exchange of threonine to methionine (CRMP1A (p.T427M, NP 001014809.1) and CRMP1B (p.T313M, NP 001304.1)); the variant in proband 3 (P3) in exon 6 c.1052T>C (NM_001014809.2) leads to an exchange of phenyl alanine to serine (CRMP1A (p.F351S, NP_001014809.1) and CRMP1B (p.F237S, NP 001304.1)). C. Multi-species sequence alignment localizes the variants in the highly conserved area of CRMP1. **D.** The short form CRMP1 monomer is composed of three structural parts, an N-terminally located 7 β-strands forming two β-sheets (depicted in blue), followed by a linker β -strand (yellow) connecting to the central α/β -barrel (cyan/magenta) formed by 7 repeats. Inserted after repeat 4 are 2 additional α-helices (gray) E. CRMP1 assembles into tetramers. The relevant sites of mutation T313M, P475L and F237S are indicated as sphere model, with the T313 and F237 located in the central channel in the vicinity of the interaction sites and P475L is locates at the beginning of the C-terminal helix and oriented towards the adjacent molecules. F. The mutation P475L reveals serious clashes with neighboring residues (red hexagonals) which may be accounted for by a shift of the helix as shown in (G). H. Detailed representation of the structural vicinity of the T313M (yellow) to the ligand-binding cavity (magenta). I. Magnified view of interface 1 tilted 90 ° backwards complex with respect to panel E highlighting the arrangement of the two phenylalanines at position 237 from the neighboring units. The exchange of phenylalanine with hydrophobic

549

550

551

552

553

554

555

556

557

558

559

560

561

562

563

564

565

566

567

568

569

570

571

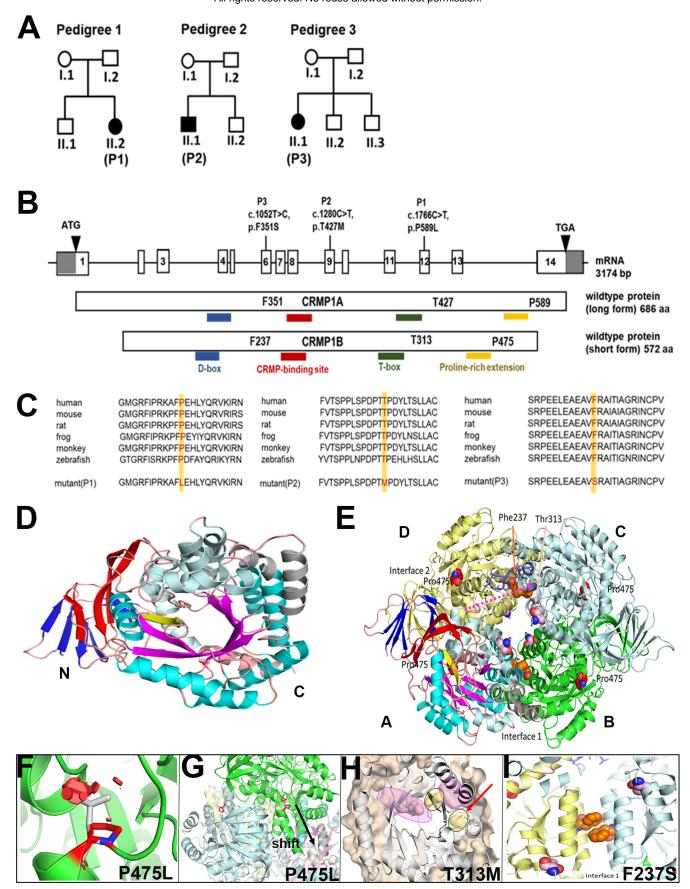
572

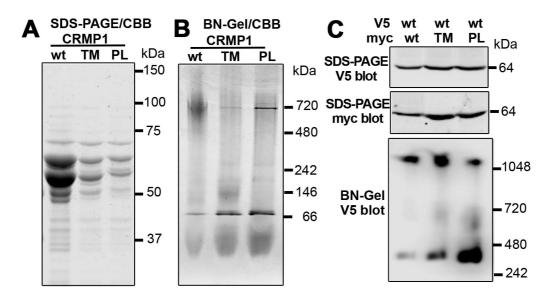
residues to serine with hydrophilic side chain interferes with the stability of the interaction in interface 1. Fig 2. Attenuated oligomer formation of CRMP1-P475L and CRMP1B-T313M mutants. A. Purified CRMP1B-wildtype, -T313M, and -P475L recombinant proteins on SDS- PAGE stained with CBB. GST-tagged CRMP1 were expressed in E. coli and purified through the binding to glutathione resin and the digestion with PreScission protease. Equal volume (2.5 μl) of the purified specimens, which were prepared in the same condition, were loaded on the gel. The yield of the mutants was less than that of CRMP1-wildtype as shown in panel. Two major 64 kDa and 60 kDa bands in the preparations are full-length and truncated form, respectively. B. Estimation of the multimeric state under native condition. Bacterially expressed and purified CRMP1B specimens (5 g) were electrophoresed on NativePAGE Novex 4-16% Bis-Tris gel in the presence of CBB-G250. The gel was stained with CBB-R250 to visualize separated proteins. CRMP1B-wildtype exhibited major 720 kDa and minor 70 kDa bands, which respectively represent homo-oligomer and monomer. In contrast, CRMP1B-T313M and -P475L showed predominant 70 kDa bands, suggesting that the mutations may interfere with the homo-oligomerization of CRMP1. C. Dominant negative effect of T313M and P475L mutant on the oligomerization of CRMP1B-wildtype. HEK293T cells co-expressing V5-CRMP1B-wildtype and either one of myc-CRMP1B-wildtype, -T313M, or -P475L were analyzed. Anti-V5 and anti-myc immunoblot analyses of the specimens subjected to SDS-PAGE showed that the expression level of V5-CRMP1 and myc-CRMP1 in each condition was similar extent (upper and middle panels). Anti-V5 immunoblot analysis of these specimens on Blue-Native gel electrophoresis is shown (lower panel). Coexpression of V5-CRMP1B-wildtype and myc-CRMP1B-wildtype exhibited major 1100 kDa and minor 360 kDa V5-reactive bands. In contrast, co-expression of myc-CRMP1B-T313M

or -P475L increased the lower (360 kDa) V5-reactive band. This suggests that co-expression

573 of these mutants may interfere with multimer formation of V5-CRMP1B-wildtype. 574 Abbreviations: CRMP1B-wildtype, wt; CRMP1B-T313M, TM; CRMP1B-P475L, PL 575 Fig 3. Attenuated neurite outgrowth by the ectopic expression of CRMP1B- P475L and 576 CRMP1B-T313M mutants. A-D. Representative images of the neurons expressing V5-CRMP1B-wildtype (A), -T313M (B), -P475L (C), or tdTomato (D). Transfected neurons 577 578 were visualized by anti-V5 immunostaining or tdTomato expression (red) and anti-MAP2 579 immunostaining (green). The longest primary neurites of the neurons expressing V5-580 CRMP1B-T313M or -P475L were shorter than those of the neurons transfected with V5-CRMP1B-wildtype or tdTomato. Scale bars, 100 µm. E. Longest primary neurite length. The 581 582 length of the longest primary neurite from V5- or tdTomato-positive neurons was scored in 583 each condition. The graph represents average ± SEM with individual values from four 584 independent experiments. The number of examined neurons in each condition is CRMP1B-585 wildtype, 66; -T313M, 64; -P475L, 49; tdTomato, 73. Data were analyzed by one-way 586 **ANOVA** followed Tukey's **p< .01, ***p by post-hoc < 0.001. test.

Author contributions. AMK and FN were responsible for project conception. AMK, MV, BD analyzed and interpreted patient's clinical data. LLB and KLM contributed clinical information by gathering clinical information and written informed consents. HH, NL, APAS, JL, TR performed WES and bioinformatics data analysis. ER performed Sanger sequencing and segregation analysis. NA, KT and FN performed functional experiments. AD performed structural prediction analysis. ER and AMK drafted the manuscript that was revised and accepted by all coauthors.





V5/tdTomato MAP2